

# Soil Micromorphology for Modeling Spatial on Landslide Susceptibility Mapping A Case Study in Kelara Subwatershed, Jeneponto Regency of South Sulawesi, Indonesia

Asmita Ahmad (✉ [asmita.ahmad@agri.unhas.ac.id](mailto:asmita.ahmad@agri.unhas.ac.id))

Universitas Hasanuddin Fakultas Pertanian <https://orcid.org/0000-0002-0302-6391>

**Meutia Farida**

Hasanuddin University: Universitas Hasanuddin

**Nirmala Juita**

Hasanuddin University: Universitas Hasanuddin

**Muh Jayadi**

Hasanuddin University: Universitas Hasanuddin

---

## Research Article

**Keywords:** plane voids, clay, soil, micromorphology, landslide

**Posted Date:** December 15th, 2022

**DOI:** <https://doi.org/10.21203/rs.3.rs-2329399/v1>

**License:**  This work is licensed under a Creative Commons Attribution 4.0 International License. [Read Full License](#)

---

**Version of Record:** A version of this preprint was published at Natural Hazards on June 21st, 2023. See the published version at <https://doi.org/10.1007/s11069-023-06063-1>.

## Abstract

Most of the results of classifying the level of susceptibility show different results, where landslides are more common in areas with a relatively high to moderate susceptibility class compared to those with a high susceptibility class. Differences in methods result in differences in the susceptibility maps resulting from the parameters that cause the tested landslides. The Spatial Regression Model can precisely interpret the relationship between several landslide parameters and events and shows better data accuracy than other methods. Utilization of soil micromorphological parameter data in mapping the level of susceptibility of the soil that triggers landslides with a Spatial Regression model so that the resulting susceptibility map can be more accurate. The soil parameter test method was carried out using a split-plot design with land use as the main plot, slope as a sub-plot, and soil physics (permeability, bulk density, and porosity) as a sub-sub-plot with three replications. Spatial modeling is done through regression analysis using ordinary least squares. The first test analysis was carried out with general parameters: lithology, rainfall, slope, land cover/land use, and population, while the second test was with parameters: lithology, rainfall, slope, land cover/land use, population, soil organic carbon, texture, erodibility and soil micromorphology. Classification of vulnerable classes using the natural breaks method. The interaction between the type of land use, slope, and physical properties of the soil on the occurrence of landslides at the study site shows a strong relationship with a significant  $p$ -value = 0.043 less than the  $\alpha$  5% level. Increased land use by the community has triggered the formation of soil micromorphology in the form of plane voids, cross-striated and grano-striated, which can trigger internal shifts (micro-shifts) in the soil body. The landslide susceptibility map at the study site is divided into seven spatial susceptibility classes: extremely low, very low, low, moderate, high, very high, and extremely high. Spatial modeling with OLS shows that the independent factors in the form of lithology, rainfall, slope, land cover/land use, and population only get an  $R^2$  value of 30.8%. Adding landslide independent parameter data in the form of soil organic carbon factor, texture, erodibility, and soil micromorphology produces a spatial model of landslide susceptibility with an increase in the accuracy value of  $R^2$  by 66.66%. The spatial model shows a high level of consistency with very significant soil micromorphology at a  $p$ -value < 0.01. The resulting spatial model is more accurate, where the high susceptibility class has a more significant number of landslide events, and landslides decrease according to the class.

## Introduction

Landslide susceptibility mapping has been carried out in many regions of the world to classify landslide events and disaster mitigation. In general, landslide susceptibility parameters use many geological factors, especially lithology and structural disturbances, climatic factors, especially rainfall, slope factors, land cover and land use factors, distance factors from rivers, landform forms, population numbers, and soil type factors (Bachri et al. 2020; Canavesi et al. 2020; Batar and Watanabe 2021; Zou and Zheng 2022). Parameters for landslide susceptibility mapping continue to grow by incorporating the latest data such as; soil erodibility, soil erosion value, soil carbon content, and soil depth (Mwaniki et al. 2015; Baruah et al. 2019). The simulation results of landslide vulnerability parameters in the Mesima Basin region in the Calabria region in Southern Italy show the accuracy of processing data from the effects of overlaying these data with real/actual conditions in the field (Conforti and Ietto 2021). Likewise, the simulation results by (Oh et al. 2017) in the Yongin region, Korea, show the accuracy of landslide occurrence data in very high susceptibility class areas. But most of the results of classifying the level of susceptibility show different results, where landslides are more common in areas with a relatively high to moderate susceptibility class than those with a high susceptibility class (Achu et al. 2020). Delineated regions are prone to experiencing fewer landslides compared to areas that are prone to even slightly prone (Canavesi et al. 2020; Sonker et al. 2021).

Differences in methods can be one factor that makes the resulting spatial model of the susceptibility map inaccurate from the parameters that cause the tested landslides (Lv et al. 2022). The semi-quantitative AHP method (Psomiadis et al., 2020) in Chania prefecture on Crete Island shows that many landslides occur in areas in the moderate to low vulnerability class. The AHP method provides good accuracy in identifying landslide events, especially on a regional scale (Roy and Saha 2019). The different levels of accuracy of the methods used can give different results in mapping landslide susceptibility, where the AHP method has an accuracy of 78.4%. In comparison, the spatial regression analysis method achieves an accuracy rate of 80-83.4% (Zhu and Huang 2006; Xiong et al. 2017). Mapping using the Frequency ratio can reach 71–89% accuracy (Oh et al. 2017; Thapa and Bhandari 2019). The Spatial Regression Model can precisely interpret the relationship between landslide parameters and landslide events (Raja et al. 2016; Xiong et al. 2017) and has been proven to be one of the most reliable spatial modeling approaches (Hemasinghe et al. 2018).

In addition, the difference in the landslide parameters also influences the resulting spatial model (Bhutia et al. 2020; Małka 2021). Adding data on clay fraction and bulk density as parameters in mapping landslide susceptibility has increased the accuracy of map data, especially in tropical areas (Sulaiman et al. 2017). Increasing soil clay fraction has also been shown to increase soil's erodibility

against landslides in the Kelara Sub-watershed (Ahmad et al. 2022b). Previous studies have proven the formation of planar planes and microstructures in landslide-prone areas (Yurong et al. 2005; Ahmad et al. 2022a), and it is not formed in locations categorized as high class of landslide susceptibility with the AHP method (Amin et al. 2021). So it is necessary to add soil micromorphological parameters in mapping the level of susceptibility of the soil that triggers landslides using the spatial regression model so that the resulting susceptibility map data can be accurate in determining the susceptibility class.

## Study Site

The study site located in Kelara Subwatershed, Rumbia District, Jeneponto Regency, with the coordinates are at 119°48'0" E – 19°57'0" E and 5°23'0" S – 5°32'0" S. The area of the Kelara Sub-watershed is 8,912.62 ha (Fig. 1). The average annual rainfall for 20 years (2000–2020) is 2552.45 mm/year (Ahmad et al. 2022a). Land cover in the study area consisted of shrubs at 0.27%, forest at 1.82%, settlement at 1.73%, dryland farming at 9.80%, mixed dryland farming at 77.66%, rice fields at 7.96%, and bareland at 0.72%. Landslides have occurred several times at the study site both in the past and present (Fig. 2).

## Methods

### Soil sampling and analysis

Landslides occur on various slopes, mostly on slopes > 25%, and can also occur on slopes < 25%. (Brahmantyo and Sadisun 2006; Achu et al. 2020; Çellek 2020; Wen et al. 2021). Soil sampling was carried out on the topsoil (0-20cm) and subsoil (> 20cm) layers with slopes < 25% and > 25% at the different land cover. Soil samples from topsoil and subsoil were analyzed for micromorphology, while soil samples from the subsoil were analyzed for the statistical test. There are 90 undisturbed soil samples and 30 disturbed soil. Soil permeability, bulk density, porosity, and texture were analyzed and calculated with BPT Procedure (BPT 2005). C-Organic was analyzed with Walkley and black method (Food and Agriculture Organization of the United Nations 2019), soil erodibility was calculated, and classification with Wischmeier and Smith (Wischmeier and Smith 1978) and Arsyad (Arsyad 2011). Classification of landcover data from Ministry of Environment and Forestry (<http://www.indonesia-geospatial.com>). Rainfall data from climate hazard group infrared precipitation with the station (CHIRPS) (<http://www.chc.ucsb.edu/data/chrips>). The result of soil organic, soil erodibility, and rainfall in spatial were built with the kriging method (Mesić Kiš 2016).

### Statistical analysis

The relationship between physical characteristics of soil, land use, and slope to determine landslide susceptibility was analyzed using a split-split plot design with three replications. Soil samples were taken on five land uses (corn plant, mixed plant, paddy fields, forests, and horticultural crops) as the main plot, two slope classes (< 25% and > 25%) as a subplot, and three soil physical properties (bulk density, porosity, and permeability) as sub-sub plot. The total of treatments was 90 combinations.

The equation for a split-split plot design (Gomez and Gomez 1984) with three replications is:

$$Y_{ijkh} = \mu + \tau_i + \beta_j + (\tau\beta)_{ij} + \gamma_k + (\beta\gamma)_{jk} + (\tau\beta\gamma)_{jkh} + \delta_h + (\beta\delta)_{jh} + (\gamma\delta)_{kh} + (\beta\gamma\delta)_{jkh} + \epsilon_{ijkh}$$

4

for: i = 1, 2, ..., r j = 1, 2, ..., a k = 1, 2, ..., b h = 1, 2, ..., c

Where:

$Y_{ijkh}$  : the value of observations in the i group, the A to j factor, the B to k factor, and the C to h factor

$\mu$  : average treatment

$\tau_i$  : influence of the group to i

$\beta_j$  : influence of A factor to j

$(\tau\beta)_{ij}$  : main plot error to i and A factor to j

$\gamma_k$  : influence B factor to k

$(\beta\gamma)_{jk}$  : interaction A factor to j and B factor to k

$(\tau\beta\gamma)_{ijk}$  : subplot error to i, A factor to j and k, and B factor to k

$\delta_h$  : influence of C factor to h

$(\beta\delta)_{jh}$  : interaction A factor to j and C factor to h

$(\gamma\delta)_{kh}$  : interaction B factor to k and C factor to h

$(\beta\gamma\delta)_{jkh}$  : interaction A factor to j, B factor to k, and C factor to h

$\epsilon_{ijkh}$  : random effect of sub-sub plot to i group, A factor to j, B factor to k, and C factor to h

The statistical analysis was performed with SPSS 17.0. A further test was performed with LSD test if the ANOVA result was significant at  $\alpha$  5%.

## Soil micromorphology analysis

The thin section follows the Benyarku and Stoops (2005) procedures. Identification of soil micromorphology using a polarizing microscope using the method of (Kerr 1959), (FitzPatrick 1993), and (Stoops 2003). Observations were made on the appearance of plane-polarized light (ppl) and crossed-polarized light (xpl).

## Regression Analysis

Ordinary Least Squares (OLR) are used to spatially map the level of landslide susceptibility in the Kelara Subwatershed area in Rumbia District, Jeneponto Regency. The OLR model is an appropriate model for a large number of independent variables (Scott and Pratt 2009). The OLR model was processed using Arc-GIS 10.3 software, with the (Scott and Pratt 2009) equations:

$$y = \beta_0 + \beta_1x_1 + \beta_2x_2 + \dots + \beta_nx_n + \epsilon$$

Where;

Y is a dependent variable

$\beta$  is coefficients

x is explanatory variables

$\epsilon$  is random error term/residuals

The first test analysis was carried out with general parameters: lithology, rainfall, slope, land cover/land use, and population. The second test is done with parameters: lithology, rainfall, slope, land cover/land use, population, soil organic carbon, texture, erodibility, and soil micromorphology. The results of the OLR spatial analysis are then classified using the natural break method, which is very applicable for classifying uneven data and classifying landslide susceptibility maps into different categories bearing in mind the similarity of embedded data values. (Wubalem 2021).

## Result

### Soil characteristics

The soil bulk density value on mixed plant, paddy field, and forest land use is higher on slopes > 25% with the slowest soil permeability class (Arsyad 2010), on mixed plant land use of 0.42 cm/hour (Table 1), which can increase soil susceptibility to landslides. Lowland rice plants are dominant on slopes of 0–8% with a bulk density value of 1.22 g/cm<sup>3</sup> belonging to the compact soil category (nrm 2021), which does not trigger landslide events but can trigger flooding events in the research location.

Table 1  
Relationship between soil physical properties and land use

| Land Use      | Slope | Bulk Density (g/cm <sup>3</sup> ) |      |      |         | Porosity (%) |       |       |           | Permeability (cm/hour) |      |      |         |
|---------------|-------|-----------------------------------|------|------|---------|--------------|-------|-------|-----------|------------------------|------|------|---------|
|               |       | I                                 | II   | III  | average | I            | II    | III   | rata-rata | I                      | II   | III  | average |
| Corn          | < 25% | 1.15                              | 1.23 | 1.19 | 1.19    | 53.93        | 52.94 | 54.03 | 53.63     | 0.99                   | 0.99 | 1.03 | 1.00    |
|               | > 25% | 1.05                              | 1.22 | 1.20 | 1.16    | 57.99        | 51.63 | 51.16 | 53.59     | 0.99                   | 1.39 | 1.31 | 1.23    |
| Mixed plant   | < 25% | 1.07                              | 1.10 | 1.11 | 1.09    | 55.03        | 54.18 | 54.06 | 54.42     | 1.16                   | 1.16 | 1.20 | 1.17    |
|               | > 25% | 1.15                              | 1.15 | 1.17 | 1.16    | 52.98        | 56.08 | 56.31 | 55.13     | 0.42                   | 0.40 | 0.44 | 0.42    |
| Paddy field   | < 25% | 1.23                              | 1.23 | 1.20 | 1.22    | 49.04        | 49.34 | 49.54 | 49.31     | 0.71                   | 0.82 | 0.87 | 0.80    |
|               | > 25% | 1.24                              | 1.22 | 1.21 | 1.22    | 50.01        | 49.15 | 49.35 | 49.50     | 0.76                   | 0.74 | 0.75 | 0.75    |
| Forest        | < 25% | 1.11                              | 1.10 | 1.11 | 1.11    | 53.15        | 53.44 | 53.62 | 53.40     | 1.22                   | 1.05 | 1.14 | 1.14    |
|               | > 25% | 1.20                              | 1.30 | 1.29 | 1.26    | 52.43        | 47.83 | 47.88 | 49.38     | 0.76                   | 1.16 | 1.18 | 1.03    |
| Horticultural | < 25% | 1.10                              | 1.19 | 1.20 | 1.16    | 58.21        | 58.40 | 58.38 | 58.33     | 1.07                   | 1.18 | 1.16 | 1.14    |
|               | > 25% | 1.13                              | 1.13 | 1.12 | 1.13    | 56.81        | 57.06 | 57.16 | 57.01     | 1.16                   | 1.18 | 1.19 | 1.18    |

The statistical test analysis showed a significant result showing the role of soil properties and land use in triggering landslide events and their interaction with a  $p$ -value = 0.000. The part of slopes < 25% and > 25% did not show a significant effect on landslide events, with a value of  $p$ -value > 0.05 (Table 2). But the interaction between the type of land use, slope, and physical properties of the soil on the occurrence of landslides at the study site shows a strong relationship with a significant  $p$ -value = 0.043 less than the  $\alpha$  5% level (Table 2). The R squared value reached 90.9%, indicating the accuracy of the relationship between the soil factor with the land use variable and the slope on the occurrence of landslides.

Table 2  
The Anova of soil physical, land use, and slope

| Tests of Between-Subjects Effects |            |                         |      |                    |           |             |
|-----------------------------------|------------|-------------------------|------|--------------------|-----------|-------------|
| Dependent Variable: Result        |            |                         |      |                    |           |             |
| Source                            |            | Type III Sum of Squares | df   | Mean Square        | F         | Sig.        |
| Intercept                         | Hypothesis | 30832.107               | 1    | 30832.107          | 48071.430 | .000        |
|                                   | Error      | 1.283                   | 2    | .641 <sup>a</sup>  |           |             |
| Land_use                          | Hypothesis | 83.518                  | 4    | 20.879             | 29.384    | .000        |
|                                   | Error      | 5.685                   | 8    | .711 <sup>b</sup>  |           |             |
| Slope                             | Hypothesis | 2.473                   | 1    | 2.473              | 4.037     | .182        |
|                                   | Error      | 1.225                   | 2    | .613 <sup>c</sup>  |           |             |
| Land_use * Slope                  | Hypothesis | 6.297                   | 4    | 1.574              | 1.731     | .160        |
|                                   | Error      | 40.011                  | 44   | .909 <sup>d</sup>  |           |             |
| Soil_Physic                       | Hypothesis | 54690.968               | 2    | 27345.484          | 26900.519 | .000        |
|                                   | Error      | 4.066                   | 4    | 1.017 <sup>e</sup> |           |             |
| Slope * Soil_Physic               | Hypothesis | 3.696                   | 2    | 1.848              | 2.032     | .143        |
|                                   | Error      | 40.011                  | 44   | .909 <sup>d</sup>  |           |             |
| Land_use * Soil_Physic            | Hypothesis | 158.256                 | 8    | 19.782             | 21.754    | .000        |
|                                   | Error      | 40.011                  | 44   | .909 <sup>d</sup>  |           |             |
| Land_use * Slope * Soil_Physic    | Hypothesis | 16.221                  | 8    | 2.028              | 2.230     | <b>.043</b> |
|                                   | Error      | 40.011                  | 44   | .909 <sup>d</sup>  |           |             |
| Rep                               | Hypothesis | 1.283                   | 2    | .641               | 1.231     | .652        |
|                                   | Error      | .242                    | .465 | .521 <sup>f</sup>  |           |             |
| Land_use * Rep                    | Hypothesis | 5.685                   | 8    | .711               | .781      | .621        |
|                                   | Error      | 40.011                  | 44   | .909 <sup>d</sup>  |           |             |
| Slope * Rep                       | Hypothesis | 1.225                   | 2    | .613               | .674      | .515        |
|                                   | Error      | 40.011                  | 44   | .909 <sup>d</sup>  |           |             |
| Soil_Physic * Rep                 | Hypothesis | 4.066                   | 4    | 1.017              | 1.118     | .360        |
|                                   | Error      | 40.011                  | 44   | .909 <sup>d</sup>  |           |             |

Further tests with LSD showed that almost all land uses showed an increase in BD values either on slopes < 25% or > 25%, directly proportional to the decrease in soil permeability in the slow to very slow category (Fig. 3). But inversely proportional to the porosity of the soil, which is still in the good category, it can trigger an increase in soil saturation which triggers landslides on slopes < 25% and on slopes > 25%. Increasing land use by communities and collaborating with global climate change has reduced the carrying capacity of the soil in stabilizing slopes and triggering landslides and flash floods at the study site.

## Soil Micromorphological Characteristics Associated With Landslides

The micromorphological characteristics of the soil that can trigger landslides are the formation of plane voids (micro cracks), striated b-fabric, and a high percentage of clay fractions which have reduced soil resistance (Yurong et al. 2006; Ahmad et al. 2018). The formation of plane voids due to soil swell activity can be used as one of the parameters in assessing the potential for landslides (Ahmad et al. 2022a).

The micromorphological appearance of the soil in lowland rice of land use on slopes of 0–8% shows the formation of plane voids due to the shrinking-swelling of soil, which contains clay fraction of 43–51%, grano-striated, and cross-striated b-fabric (Fig. 4). Collaboration of paddy fields and slopes of 0–8% cannot trigger a landslide.

The appearance of the soil micromorphology in mixed land use (coffee-cacao-banana-timber) showed an increase in the clay fraction of 34–42% at the topsoil. Some minerals have undergone mesomorphous weathering to become clay, and clay coatings are found at the edges of mineral crystals (Fig. 5). Increasing the clay content in the subsoil (46–60%) has increased bulk density and decreased soil permeability (Table 1), with weathering of minerals in the subsoil layer showing catamorphic weathering of minerals. Most of the minerals have been crushed and weathered to form clay minerals accompanied by the intensive formation of planar planes, grano-striated, and striated b-fabric (Figs. 6 and 7).

The clay fraction in the subsoil is higher than in topsoil, especially in the land use of mixed gardens, forests, and lowland rice. Land management, mineral type, and increased rainfall resulted in a more intensive weathering process. At the same time, the porosity was still in good condition. Still, it had decreased permeability in the subsoil, making the soil easily saturated and triggering landslides on slopes < 25% and > 25%. The formation of cross-striated and striated grano can trigger an internal shift (micro-shift) in the soil body.

## General Parameter For Landslide Susceptibility Mapping

The most common parameters used to assess landslides used by experts in determining landslide susceptibility classes are the lithology factor, rainfall factor, slope factor, land cover, and land use factor, and population. (Bachri et al. 2020; Batar and Watanabe 2021; Zou and Zheng 2022) (Fig. 8). The OLS analysis results show that the lithology parameter is an essential factor causing an increase in soil susceptibility at the study site with a significant Robust\_Probability value at  $p$ -value < 0.01 (Table 3). This is in accordance with the results of research from Hong et al. (Hong et al. 2017), which shows that lithology parameters trigger the dominant landslide events.

Table 3  
The OLS statistic of landslide susceptibility mapping

| Variable                   | Coefficient [a] | StdError | t-Statistic | Probability (b) | Robust_SE | Robust_t  | Robust_Pr [b] | VIF [c]  |
|----------------------------|-----------------|----------|-------------|-----------------|-----------|-----------|---------------|----------|
| Intercept                  | 2.184028        | 2.090371 | 1.044804    | 0.313817        | 1.513412  | 1.443115  | 0.170994      | —        |
| Population                 | 0.000054        | 0.000093 | 0.579704    | 0.571328        | 0.000077  | 0.702179  | 0.494075      | 1.137159 |
| Lithology                  | -0.112894       | 0.056641 | -1.993132   | 0.06611         | 0.02333   | -4.839021 | 0.000264*     | 1.221578 |
| LULC                       | 0.015147        | 0.048223 | 0.314097    | 0.758083        | 0.016231  | 0.933167  | 0.366546      | 1.067081 |
| Slope                      | 0.005504        | 0.01915  | 0.287429    | 0.777997        | 0.012724  | 0.43258   | 0.671914      | 1.174942 |
| Rainfall                   | 0.000594        | 0.000535 | 1.111308    | 0.285156        | 0.000443  | 1.342139  | 0.200916      | 1.12064  |
| *significant on $p < 0.01$ |                 |          |             |                 |           |           |               |          |

The Koenker value (BP) statistic is 0.588275, which is greater than  $p$ -value > 0.01, showing that the model relationship is relatively consistent. But the Jarque-Bera Statistic value is 0.010880 with a  $p$ -value < 0.01, indicating the prediction model is biased. So the  $R^2$  value is only 30.8%, meaning that there are still 69.2% external factors that influence the dependent aspect, the results of mapping the soil susceptibility do not provide accurate results in predicting the level of susceptibility to landslides in the study location. This shows that the most common parameters used to determine the class of landslide susceptibility have not been able to provide an accurate model in the field of landslide events that occur.

## Specific Parameters For Landslide Susceptibility Mapping

Soil parameters have been used by several researchers in assessing landslide susceptibility, especially soil texture, macro-micro porosity, and erodibility (Fonseca et al. 2017b; Conforti and Letto 2021). The addition of soil micromorphology data in the form of plane voids has significantly affected the physical occurrence of landslides at the study site (Ahmad et al. 2022a). The spatially adding soil organic carbon, soil texture, soil erodibility, and soil micromorphology data (Fig. 9) to assess landslide susceptibility is expected to provide more accuracy and validity in producing susceptibility maps. The results of the OLS regression analysis are presented in Table 4.

Table 4  
The OLS statistic of landslide susceptibility mapping

| Variable                   | Coefficient [a] | StdError | t-Statistic | Probability (b) | Robust_SE | Robust_t  | Robust_Pr [b] | VIF [c]  |
|----------------------------|-----------------|----------|-------------|-----------------|-----------|-----------|---------------|----------|
| Intercept                  | -1.63055        | 7.828637 | -0.20828    | 0.839206        | 8.282964  | -0.196856 | 0.847899      | ——       |
| Population                 | 0.005859        | 0.05316  | 0.110206    | 0.914438        | 0.049626  | 0.118054  | 0.908374      | 2.451664 |
| C-Organic                  | -0.172078       | 0.16288  | -1.056466   | 0.315615        | 0.1682    | -1.023053 | 0.330397      | 1.110746 |
| Soil-Erodibility           | 2.124802        | 0.843201 | 2.519924    | 0.030381*       | 0.718342  | 2.957925  | 0.014346*     | 2.173448 |
| LULC                       | 0.065958        | 0.051014 | 1.292932    | 0.225122        | 0.031907  | 2.067167  | 0.065582      | 1.668384 |
| Slope                      | 0.019528        | 0.018249 | 1.070104    | 0.309727        | 0.012665  | 1.541891  | 0.154139      | 1.703753 |
| Rainfall                   | -0.000624       | 0.000677 | -0.920981   | 0.378738        | 0.000791  | -0.788648 | 0.448597      | 2.662604 |
| Texture                    | 0.065843        | 0.183515 | 0.358786    | 0.72722         | 0.364225  | 0.723279  | 3.394234      | ——       |
| Lithology                  | 0.092355        | 0.137048 | 0.673891    | 0.515639        | 0.15826   | 0.583564  | 0.572426      | 2.714366 |
| Plane voids                | -0.000041       | 0.000018 | -2.311536   | 0.043379*       | 0.00002   | -2.061113 | 0.066251      | 1.955582 |
| *significant on $p < 0.01$ |                 |          |             |                 |           |           |               |          |

The Koenker value (BP) statistic is 0.149728, which is greater than the  $p$ -value  $> 0.01$ , showing that the model relationship is relatively consistent. The Jarque-Bera Statistic value is 0.925161 with a  $p$ -value  $> 0.01$ , which shows that the prediction model is not biased. The  $R^2$  value of 66.66% indicates that the independent factor has a significant effect on the dependent factor, so the results of soil vulnerability mapping provide more accurate results in predicting the level of landslide susceptibility in the study location. This shows that soil erodibility parameters and micromorphology, especially plane voids, can improve the accuracy of landslide susceptibility classes and provide an accurate model of landslides occurring in the field.

## Discussion

A landslide susceptibility map can provide important information regarding the potential for landslide events that may occur in an area and an overview of the area's environmental conditions. However, this map cannot determine when landslide events can occur, the type of landslide that occurs (whether it is a shallow landslide or depth landslide), the volume of the landslide, and the impact of the damage caused. Spatial landslide susceptibility maps are used to mitigate disaster events that can arise in local and regional land use planning because the impact of events can cover the entire watershed area.

The landslide susceptibility map is always assumed to occur on a high slope class  $> 25\%$  resulting from independent factors such as slope, lithology, land cover, rainfall, and population. The dominant slope and lithological parameter are assumed to be the main factors causing landslides, with rainfall triggering factors (Yu et al. 2021). However, this is a question mark in several regions where a high spatial susceptibility class has fewer landslides than a low susceptibility spatial class. Several researchers have added parameters to sharpen the resulting spatial quality so that it can approach actual conditions in the field. One of the parameters included as an independent factor in the spatial analysis is the macromorphological characteristics of the soil. The addition of soil data as a factor causing landslides raises debate because many soil parameters can become separate parameters that influence landslide events and have a spatially different impact on landslide susceptibility. (Kitutu et al. 2009) and (Liu et al. 2021) show that the soil type parameters do not significantly affect landslide events. But the value of the physical properties of the soil in the form of soil porosity, permeability, and bulk density of the soil is considered a soil factor that can affect the occurrence of landslides if it is associated with land use

cultivated by the community. (Reichenbach et al. 2014; Fonseca et al. 2017a). Statistical test results indicated significant collaboration of the type of land use, slope, and physical properties of the soil (soil porosity, bulk density, and permeability) on the occurrence of landslides at the study site (Table 2). The significance value of  $p = 0.043$  is less than the  $\alpha$  5% level, with the R squared value reaching 90.9%. Likewise, further tests show that the permeability value is in line with the bulk density value and inversely proportional to the porosity value in collaboration with increasing soil susceptibility in triggering landslide events (Fig. 3).

The impact of changes in soil properties due to intensive land use has resulted in changes in soil micromorphology. The increase in the content of the clay fraction > 46% with slow permeability has led to the formation of striated b-fabric and plane voids (micro cracks), which have reduced soil resistance both on slopes < 25% or > 25% (Yurong et al. 2006; Ahmad et al. 2018). There is a very strong relationship between an increase in the clay fraction and an increase in micro cracks in various soil types (Fattah et al. 2018). The formation of striated b-fabric in the form of clay coating and plane voids has reduced the ability of soil pore space (Vingiani et al. 2015). According to Islam et al. (Islam et al. 2022), parameters in assessing landslide susceptibility can be added according to specific locations to reduce the impact of landslide events. Simulation results performed by Bhutia et al. (Bhutia et al. 2020) state that the difference in the level of accuracy of the various landslide parameters used, while using soil parameters can increase the accuracy value by 84% in predicting landslide events. Therefore, plane voids due to swelling soil activities can be used to assess the potential for landslides at the study site.

The landslide susceptibility map at the study site is divided into seven spatial susceptibility classes: extremely low, very low, low, moderate, high, very high, and extremely high. Spatial modeling with OLS shows that the independent factors in the form of lithology, rainfall, slope, land cover/land use, and population only get an  $R^2$  value of 30.8%. This shows that the parameters used cannot provide an overview of actual conditions in the field. The locations of high landslide events are in the high susceptibility class, while in the extremely high susceptibility class, there is only one landslide event (Fig. 10). Research results from (Amin et al. 2021) at the same location in the Kelara Subwatershed with the AHP method and general parameters also show that landslide events are only found in the medium class and not at high susceptibility. This is because the data on the resulting spatial model is inconsistent due to the need for more detailed data for a larger map scale (Chalkias et al. 2014). Adding landslide independent parameter data in the form of soil organic carbon factor, texture, erodibility, and soil micromorphology simulated with general factors produces a spatial model of landslide susceptibility with an increase in the accuracy value of  $R^2$  by 66.66%. The spatial model shows a high degree of consistency with the Koenker value is 0.149728 and is very significant in soil micromorphology at  $p\text{-value} < 0.01$ . The resulting spatial model is more accurate, where the high susceptibility class has a greater number of landslide events, and landslides decrease according to the class (Fig. 11). The study's results by Achu et al. (Achu et al. 2020) also prove that a greater variety of independent factors will result in a more accurate spatial model of landslide susceptibility.

## Conclusions

Landslide is a disaster that often occurs in the Kelara Sub-watershed, Rumbia Jeneponto District, South Sulawesi, Indonesia, especially during the rainy season, which causes damage to agricultural land, settlements, and loss of life. Therefore it is crucial to accurately determine the landslide susceptibility class spatial model to reduce the damage caused. The landslide susceptibility map at the study site is divided into seven spatial susceptibility classes: extremely low, low, very low, moderate, high, very high, and extremely high. Spatial modeling with OLS shows that independent parameters such as lithology, rainfall, slope, land cover/land use, and population have an  $R^2$  value of 30.8%. The main causative factor is lithology, with the significance  $p\text{-value} = 0.000264$ . The spatial model, with the addition of independent landslide parameter data in the form of soil organic carbon factor, texture, erodibility, and micromorphology of soil, produces a spatial model of landslide susceptibility with an increase in the accuracy value of  $R^2$  by 66.66%. The main causative factor is soil micromorphology (plane voids), with a significant value of  $p = 0.043379$ . The resulting spatial model of the landslide susceptibility map is more accurate, where the high susceptibility class has a greater number of landslide events.

## Declarations

**Acknowledgments** Thanks to the Ministry of research and Technology/National Research and Innovation Agency Indonesia and the Research and Community Service (LP2M) of Universitas Hasanuddin for supporting this research

**Funding** This study was funded by the Ministry of research and Technology/National Research and Innovation Agency Indonesia

**Conflict of interest** The authors declare no competing interest

## References

1. Achu AL, Aju CD, Reghunath R (2020) Spatial modelling of shallow landslide susceptibility: a study from the southern Western Ghats region of Kerala, India. *Ann GIS* 26:113–131. <https://doi.org/10.1080/19475683.2020.1758207>
2. Ahmad A, Farida M, Juita N (2022a) Soil micromorphology of land cover in landslide Ssusceptibility area in Kelara Subwatershed, Jeneponto, Indonesia. *Asian J Plant Sci* 21:643–653. <https://doi.org/10.3923/ajps.2022.643.653>
3. Ahmad A, Farida M, Juita N, Amin N (2022b) Soil erodibility mapping for soil susceptibility in the upstream of Kelara Subwatershed in Jeneponto Regency. *IOP Conf Ser Earth Environ Sci* 986. <https://doi.org/10.1088/1755-1315/986/1/012031>
4. Ahmad A, Poch RM, Lopulisa C et al (2018) Identification of Soil Characteristic on North Toraja Landslide, Indonesia. *ARPN J Eng Appl Sci* 13:8381–8385
5. Amin N, Lias SA, Ahmad A (2021) Potential landslide-prone areas in the Kelara sub-watershed using the analytical hierarchy process method. *IOP Conf Ser Earth Environ Sci* 807:1–11. <https://doi.org/10.1088/1755-1315/807/2/022080>
6. Arsyad S (2011) *Konservasi Tanah Dan Air*. 1–19
7. Arsyad S (2010) *Konservasi Tanah & Air (Soil and Water Conservation)*. IPB Press
8. Bachri S, Shrestha RP, Yulianto F et al (2020) Mapping landform and landslide susceptibility using remote sensing, GIS and field observation in the Southern cross road, Malang Regency, East Java, Indonesia. *Geosciences* 11:1–15. <https://doi.org/10.3390/geosciences11010004>
9. Baruah S, Kumaraperumal R, Kannan B et al (2019) Soil erodibility estimation and its correlation with soil properties in Coimbatore district. *Int J Chem Stud* 7:3327–3332
10. Batar AK, Watanabe T (2021) Landslide susceptibility mapping and assessment using geospatial platforms and weights of evidence (WoE) method in the Indian himalayan region: Recent developments, gaps, and future directions. *ISPRS Int J Geo-Information* 10:1–28. <https://doi.org/10.3390/ijgi10030114>
11. Bhutia SL, Borah S, Pradhan R, Sharma B (2020) An Experiment on Parameter Selection for Landslide Susceptibility Mapping using TF-IDF. *J Phys Conf Ser* 1712:1–10. <https://doi.org/10.1088/1742-6596/1712/1/012029>
12. BPT (2005) Analisis kimia tanah, tanaman, air dan pupuk
13. Brahmantyo B, Sadisun IA(2006) Slope and Lithological Controls on Landslide Distribution on West Java, Indonesia. In: *Proceedings of International Symposium on Geotechnical Hazards: Prevention, Mitigation and Engineering Response*. pp 177–184
14. Canavesi V, Segoni S, Rosi A et al (2020) Different approaches to use morphometric attributes in landslide susceptibility mapping based on meso-scale spatial units: A Case Study in Rio de Janeiro (Brazil). *Remote Sens* 12:1–24. <https://doi.org/10.3390/rs12111826>
15. Çellek S (2020) Effect of the slope angle and its classification on Landslide. *Nat Hazards Earth Syst Sci* 1–23. <https://doi.org/10.5194/nhess-2020-87>
16. Chalkias C, Ferentinou M, Polykretis C (2014) GIS-Based Landslide Susceptibility Mapping on the Peloponnese Peninsula. *Greece Geosci* 4:176–190. <https://doi.org/10.3390/geosciences4030176>
17. Conforti M, Ietto F(2021) Modeling Shallow Landslide Susceptibility and Assessment of the Relative Importance of Predisposing Factors, through a GIS-Based Statistical Analysis. *geosciences* 11:1–28. <https://doi.org/10.3390/geosciences11080333>
18. Fattah MAF, Khurshid SHK, Ahmad RAA (2018) Soil cracking depth as influenced by soil physical properties. *J Zankoy Sulaimani* 2:105–114. <https://doi.org/10.17656/jzs.10657>
19. FitzPatrick E (1993) *Soil Microscopy And Micromorphology*. Chichester, New York, Brisbane, Toronto, Singapore
20. Fonseca LDM, Lani JL, Fernandes Filho EI et al (2017a) Variability in soil physical properties in landslide-prone areas. *Acta Sci Agron* 39:109. <https://doi.org/10.4025/actasciagron.v39i1.30561>
21. Fonseca LDM, Lani JL, Filho EIF et al (2017b) Variability in soil physical properties in landslide-prone areas. *Acta Sci - Agron* 39:109–118. <https://doi.org/10.4025/actasciagron.v39i1.30561>
22. Food and Agriculture Organization of the United Nations (2019) Standard operating procedure for soil organic carbon. Walkley-Black method
23. Gomez AA, Gomez KA(1984) *Statistical Procedures For Agricultural Research* Second Edition, Second Edi
24. Hemasinghe H, Rangali RSS, Deshapriya, Samarakoon L (2018) Landslide susceptibility mapping using logistic regression model (a case study in Badulla District, Sri Lanka). *Procedia Eng* 212:1046–1053. <https://doi.org/10.1016/j.proeng.2018.01.135>

25. Hong H, Pradhan B, Sameen MI et al (2017) Spatial prediction of rotational landslide using geographically weighted regression, logistic regression, and support vector machine models in Xing Guo area (China). *Geomatics. Nat Hazards Risk* 8:1997–2022. <https://doi.org/10.1080/19475705.2017.1403974>
26. Islam F, Riaz S, Ghaffar B et al (2022) Landslide susceptibility mapping (LSM) of Swat District, Hindu Kush Himalayan region of Pakistan, using GIS-based bivariate modeling. *Front Environ Sci* 10:1–18. <https://doi.org/10.3389/fenvs.2022.1027423>
27. Kerr P (1959) *Optical Mineralogy*, 3rd edn. McGraw-Hill Book Company, Inc
28. Kitutu MG, Muwanga A, Poesen J, Deckers JA (2009) Influence of soil properties on landslide occurrences in Bududa district, Eastern Uganda. *Afr J Agric Res* 4:611–620
29. Liu Y, Deng Z, Wang X (2021) The effects of rainfall, soil type and slope on the processes and mechanisms of rainfall-induced shallow landslides. *Appl Sci* 11:1–14. <https://doi.org/10.3390/app112411652>
30. Lv L, Chen T, Dou J, Plaza A(2022) International Journal of Applied Earth Observations and Geoinformation A hybrid ensemble-based deep-learning framework for landslide susceptibility mapping. *Int J Appl Earth Observation Geoinf* 108
31. Małka A (2021) *Landslide susceptibility mapping of Gdynia using geographic information system-based statistical models*. Springer Netherlands
32. Mesić Kiš I (2016) Comparison of ordinary and universal kriging interpolation techniques on a depth variable (a case of linear spatial trend), case study of the Šandrovac Field. *MGPB* 31:41–58. <https://doi.org/10.17794/rgn.2016.2.4>
33. Mwaniki MW, Agutu NO, Mbaka JG et al (2015) Landslide scar / soil erodibility mapping using Landsat TM / ETM + bands 7 and 3 Normalised Difference Index: A case study of central region of Kenya. *Appl Geogr* 64:108–120. <https://doi.org/10.1016/j.apgeog.2015.09.009>
34. nrm (2021) *Technical Information: Soil Physical Analysis-Getting Started*. nrm part Cawood 1:1–3
35. Oh H, Lee S, Hong S (2017) Landslide susceptibility assessment using frequency ratio technique with iterative random sampling. *J Sens* 1–21. <https://doi.org/10.1155/2017/3730913>
36. Raja NB, Çiçek I, Türkoğlu N et al (2016) Landslide susceptibility mapping of the Sera River Basin using logistic regression model. *Nat Hazards* 85:1323–1346. <https://doi.org/10.1007/s11069-016-2591-7>
37. Reichenbach P, Busca C, Mondini AC, Rossi M (2014) The Influence of Land Use Change on Landslide Susceptibility Zonation: The Briga Catchment Test Site (Messina, Italy). *Environ Manage* 54:1372–1384. <https://doi.org/10.1007/s00267-014-0357-0>
38. Roy J, Saha S (2019) Landslide susceptibility mapping using knowledge driven statistical models in Darjeeling District, West Bengal, India. *Geoenvironmental Disasters* 6:1–18. <https://doi.org/10.1186/s40677-019-0126-8>
39. Scott L, Pratt M(2009) *An introduction to using regression analysis with spatial data*. 40–43
40. Sonker I, Tripathi JN, Singh AK (2021) Landslide susceptibility zonation using geospatial technique and analytical hierarchy process in Sikkim Himalaya. *Quat Sci Adv* 4:1–17. <https://doi.org/10.1016/j.qsa.2021.100039>
41. Stoops G (2003) *Guidelines for Analysis and Description of Soil*. Soil Science Society of America, Inc
42. Sulaiman WNA, Rosli MH, Samah MAA, Kamarudin MKA (2017) Landslide susceptibility mapping: Effect of spatial resolution towards the prediction of landslide prone area in a tropical catchment. *Chiang Mai J Sci* 44:494–507
43. Thapa D, Bhandari BP (2019) GIS-Based Frequency Ratio Method for Identification of Potential Landslide Susceptible Area in the Siwalik Zone of Chatara-Barahakshetra Section, Nepal. *Open J Geol* 9:873–896. <https://doi.org/10.4236/ojg.2019.912096>
44. Vingiani S, Mele G, De Mascellis R et al (2015) Volcanic soils and landslides: A case study of the island of Ischia (southern Italy) and its relationship with other Campania events. *Solid Earth* 6:783–797. <https://doi.org/10.5194/se-6-783-2015>
45. Wen Y, Gao P, Mu X et al (2021) Experimental Study on Landslides in Terraced Fields in the Chinese Loessial Region under Extreme Rainfall. *Water* 13:1–21. <https://doi.org/10.3390/w13030270>
46. Wischmeier WH, Smith DD (1978) *Predicting rainfall erosion losses*. United States Department of Agriculture
47. Wubalem A (2021) Landslide susceptibility mapping using statistical methods in Uatzau catchment area, northwestern Ethiopia. *Geoenvironmental Disasters* 8:1–21. <https://doi.org/10.1186/s40677-020-00170-y>
48. Xiong T, Indrawan IGB, Putra DPE (2017) Landslide Susceptibility Mapping Using Analytical Hierarchy Process, Statistical Index, Index of Entropy, and Logistic Regression Approaches in the Tinalah Watershed, Yogyakarta. *J Appl Geol* 2:78–93. <https://doi.org/10.22146/jag.19983>

49. Yu X, Zhang K, Song Y et al (2021) Study on landslide susceptibility mapping based on rock–soil characteristic factors. *Sci Rep* 11:1–27. <https://doi.org/10.1038/s41598-021-94936-5>
50. Yurong HE, Chaolin L, Pei XU, Baohua Z (2005) Zonal Distribution of the Erosion-Landslide and Soil Micromorphological Features in Purple Hilly Region. *J Mt Sci* 2:42–49
51. Yurong HE, Peng CUI, Chaolin L et al (2006) Micromorphology of landslide soil Case study on the Jibazi landslide in Yunyang in the Three Gorges Region, China. *J Mt Sci* 3:147–157
52. Zhu L, Huang JF (2006) GIS-based logistic regression method for landslide susceptibility mapping in regional scale. *J Zhejiang Univ Sci* 7:2007–2017. <https://doi.org/10.1631/jzus.2006.A2007>
53. Zou Y, Zheng C (2022) A Scientometric analysis of predicting methods for identifying the environmental risks caused by landslides. *Appl Sci* 12:1–31. <https://doi.org/10.3390/app12094333>

## Figures

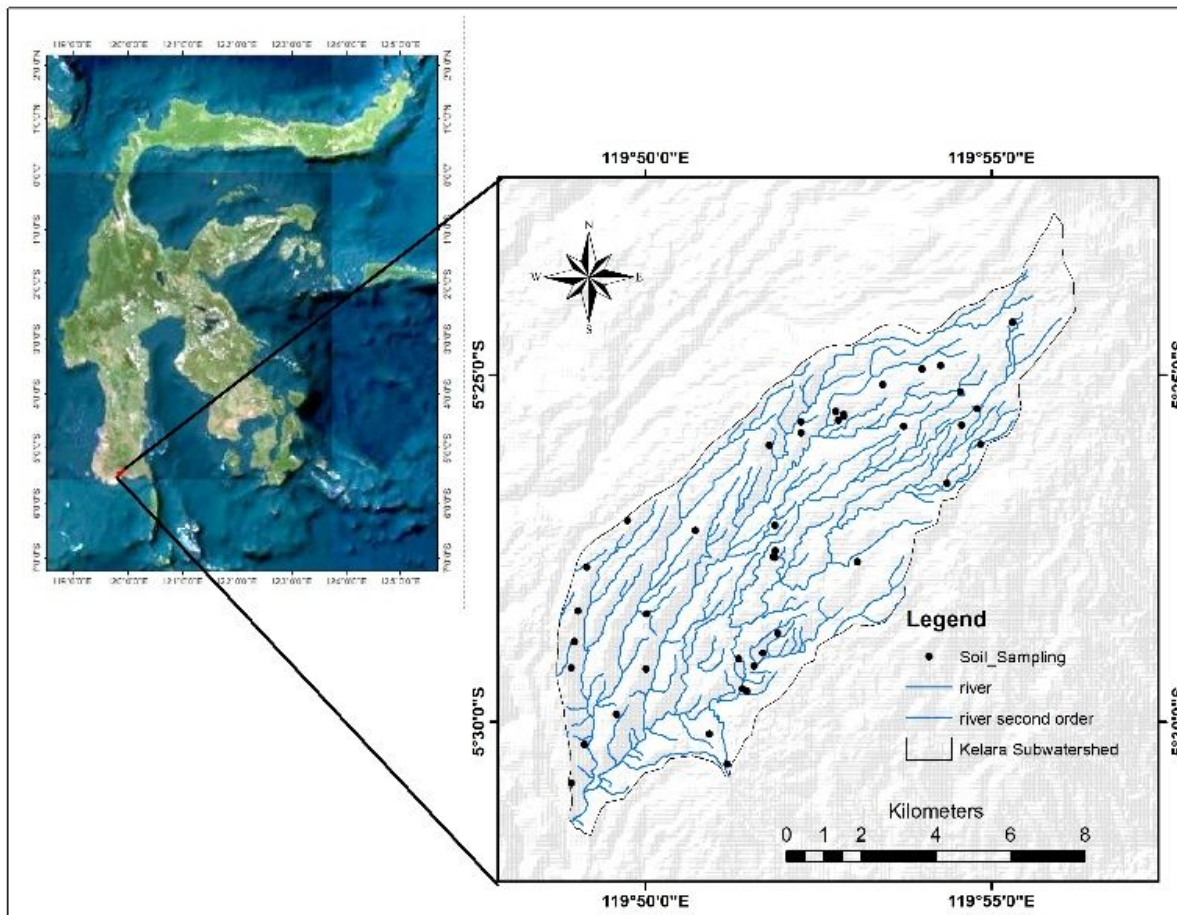


**Figure 1**

Location of the study site



Figure 2

Location of the study site

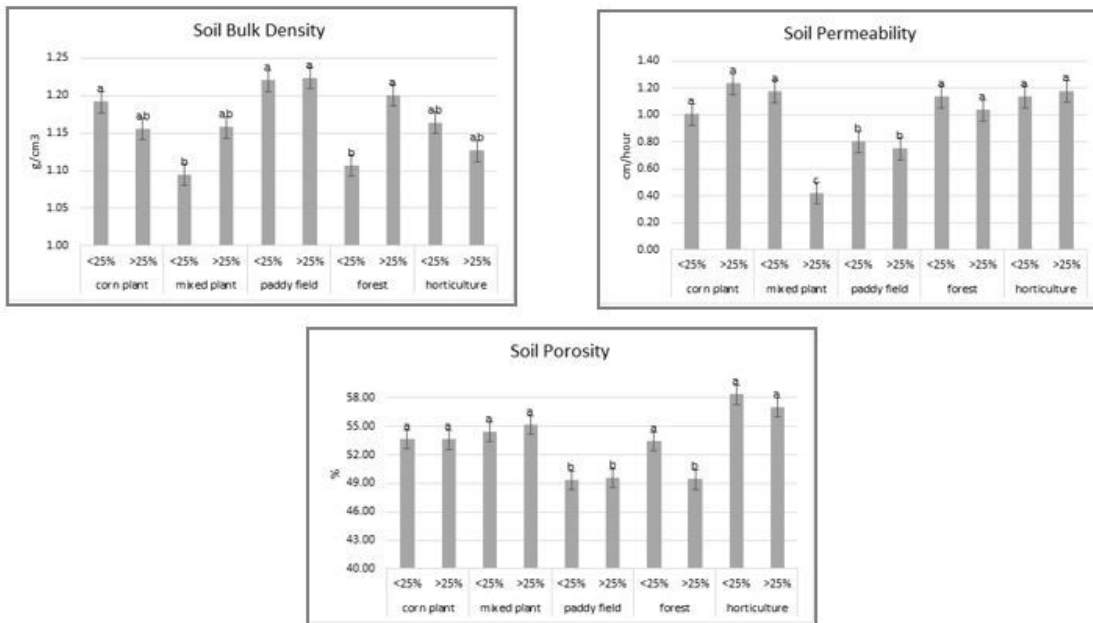
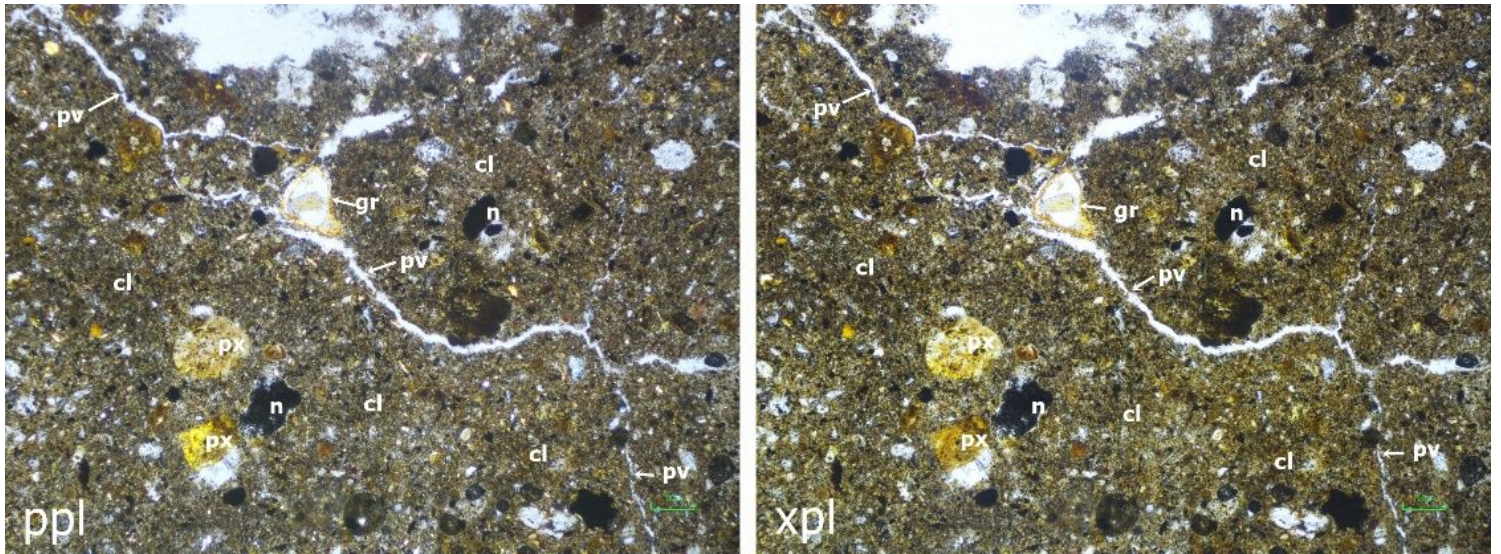


Figure 3

LSD test of soil bulk density, porosity, and permeability at slope <25% and >25% with different land use that triggers a landslide (The numbers followed by the same letter show no significant difference at a 0.05).



**Figure 4**

The micromorphological appearance of paddy soil shows the formation of planar voids (pv) due to an increase in the content of the clay (cl) fraction, grano-striated (gr), pyroxene mineral (px), and nodule (n). Size 100µm.

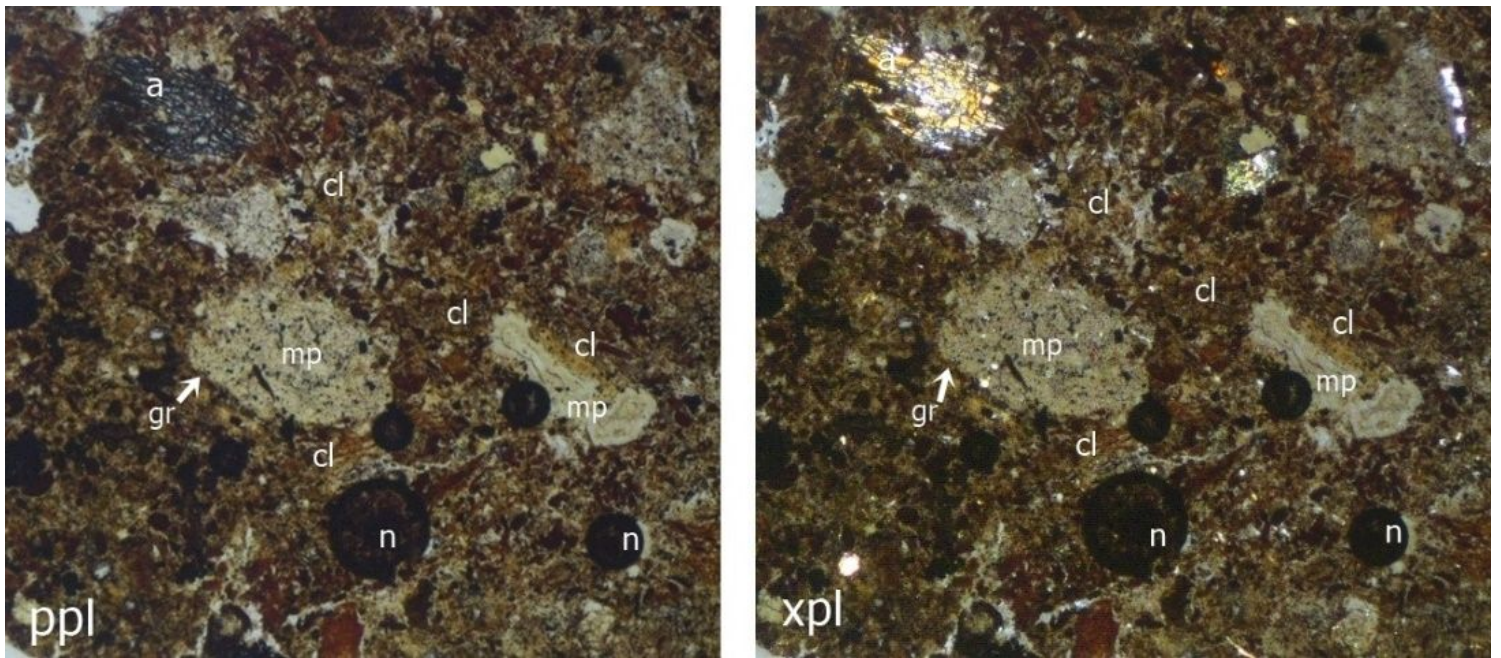


**Figure 5**

The micromorphological appearance of the soil in the topsoil at the landslide site showed an increase in clay (cl) content between mineral crystal grains. Also shows grano-striated (gr), amphibole mineral (a), mesomorphous (mp) mineral, and nodule (n). However, it did not show any planar voids, and amphibole minerals were still found as a source of soil nutrients. Size 100µm.

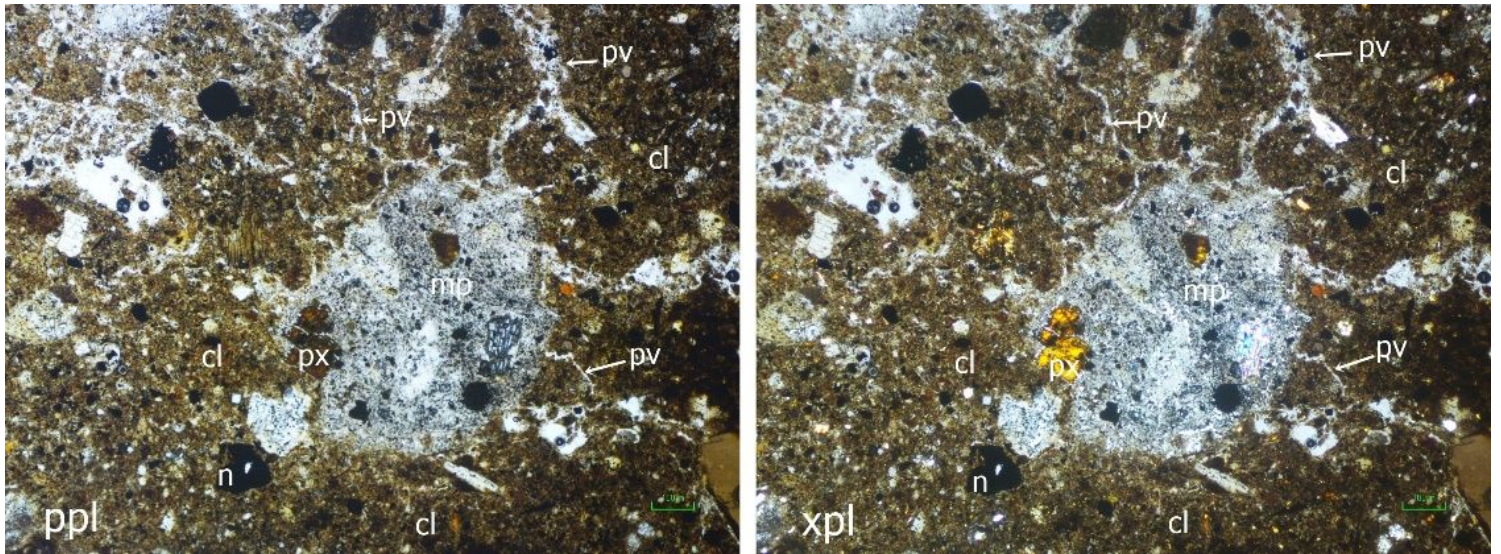


**Figure 6**

The appearance of soil micromorphology in the subsoil at the landslide site, with intensive planar voids (pv) and clay (cl) fraction formed. It also shows weathering mineral mesomorphous (mp), pyroxene mineral (px), and nodule (n). Size 100µm.

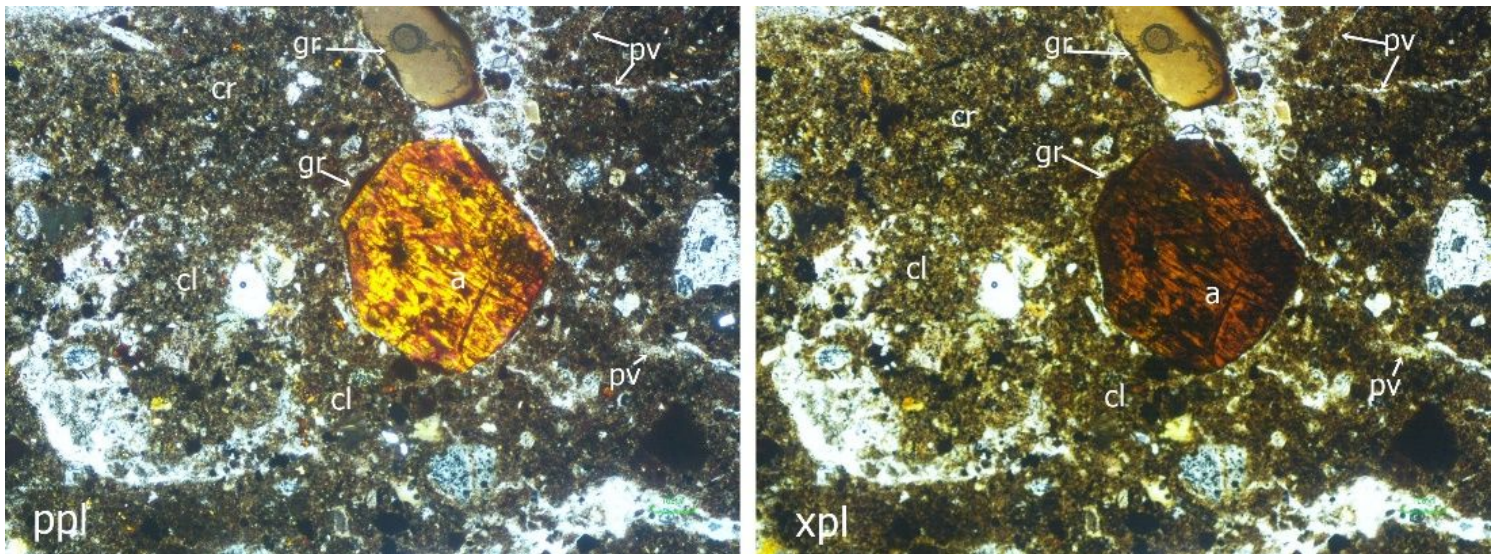


**Figure 7**

The micromorphological appearance of the subsoil in the soil at the landslide site, with the development of planar voids (pv), cross-striated (cr), grano-striated (gr), amphibole mineral (a) and intensive mineral weathering. Size 100µm.

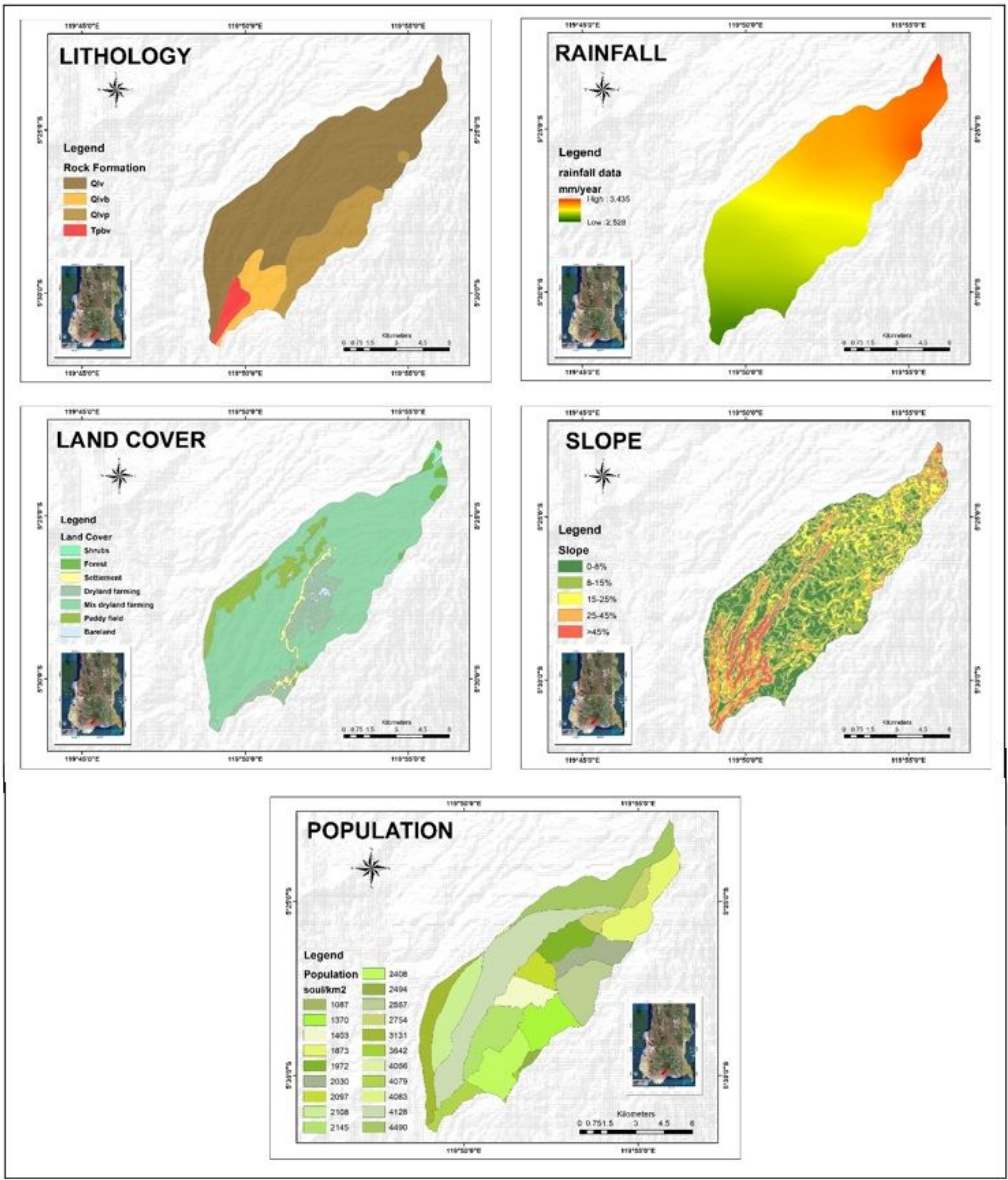


Figure 8

The general landslide-related factors in the study area

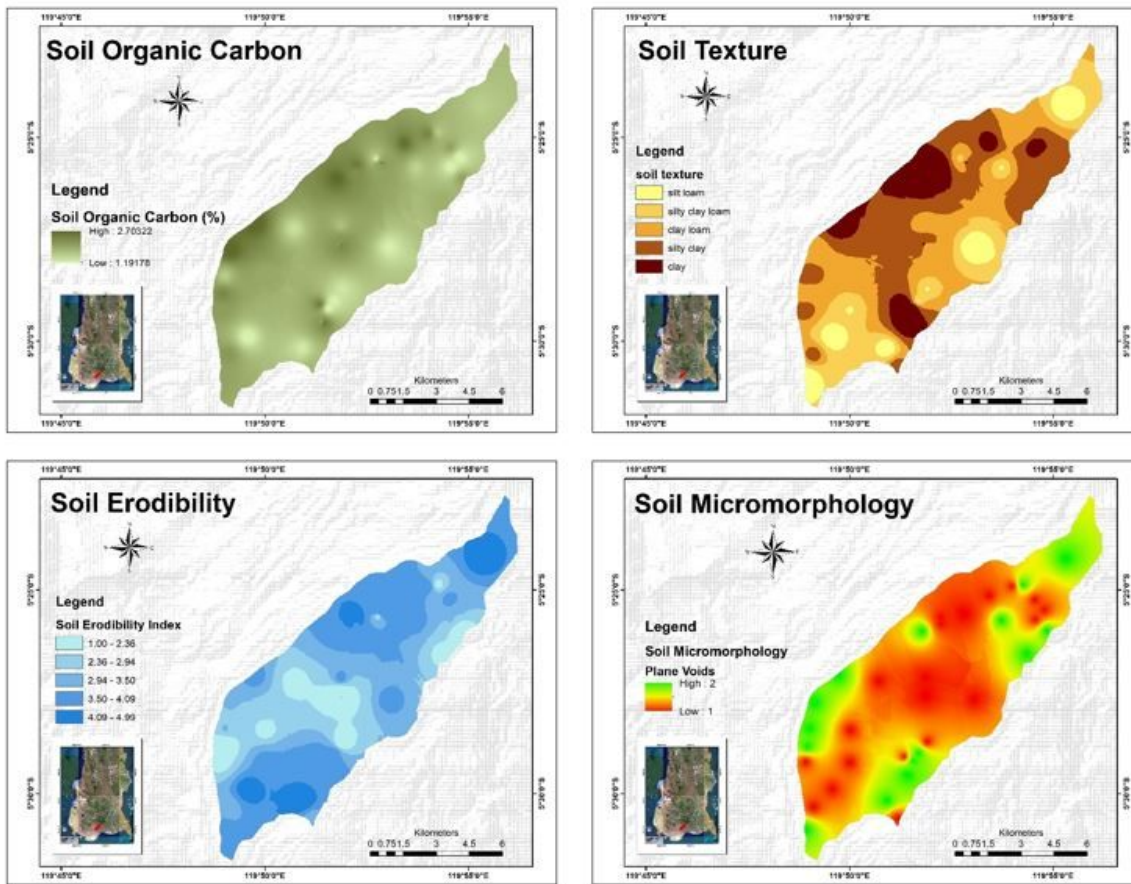


Figure 9

The Specific factors related to landslides in the study area

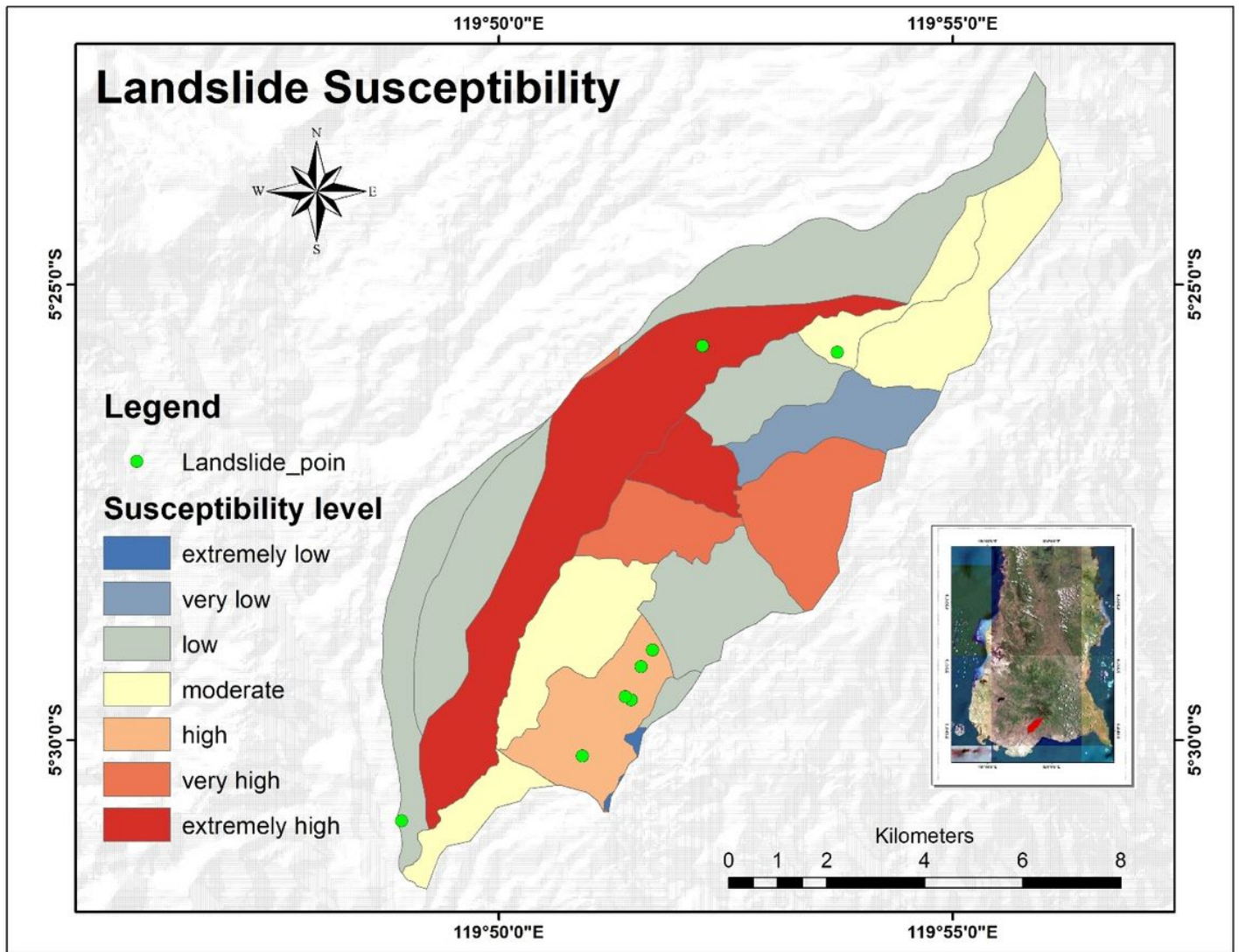


Figure 10

Landslide susceptibility mapping with the parameter of lithology, rainfall, slope, cover, and land use.

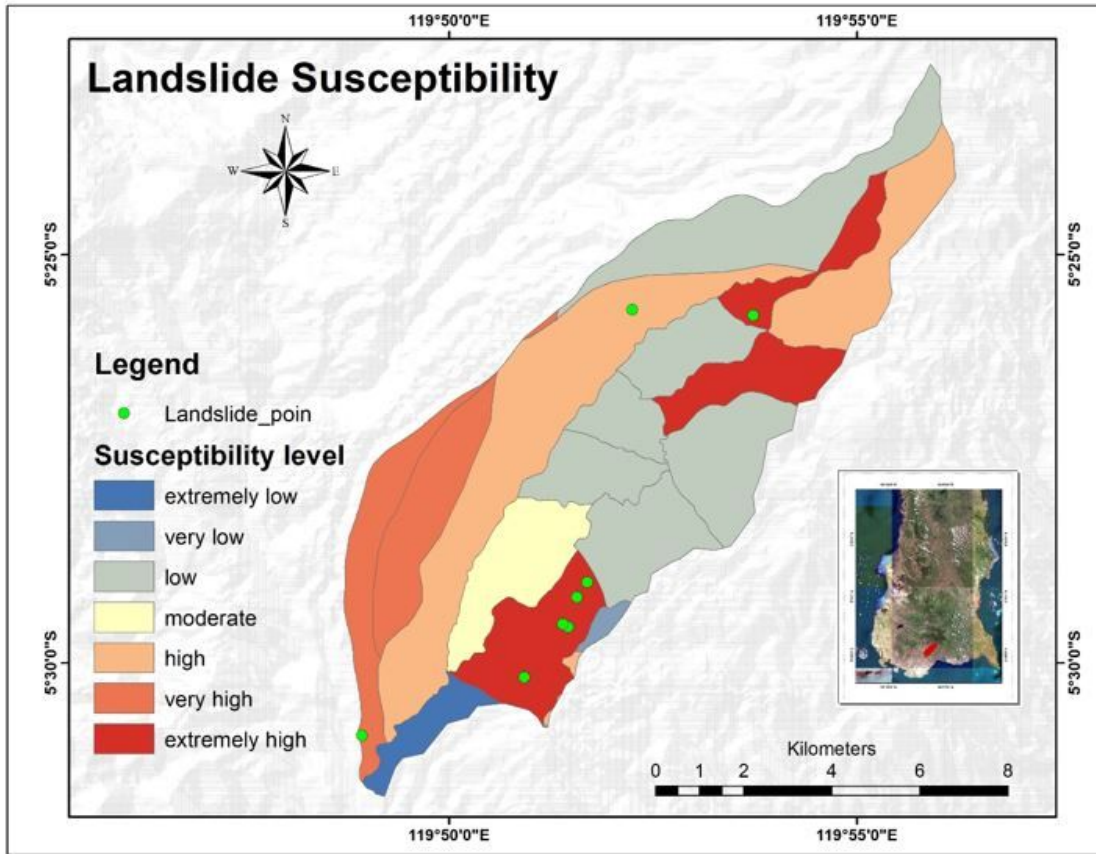


Figure 11

Landslide susceptibility mapping with the parameter of lithology, rainfall, slope, cover factor, land use, soil organic carbon, soil texture, soil erodibility, and soil micromorphology.